## Author version

Published as:

Wang, B., Ruh, M. L., Tian, A., Scotzniovsky, L., & Hwang, J. T. (2025). Large-scale MDO under uncertainty of an eVTOL aircraft using dimension reduction via global sensitivity analysis. In AIAA AVIATION FORUM AND ASCEND 2025 (Paper No. AIAA 2025-3344). https://doi.org/10.2514/6.2025-3344

BibTeX for this reference:

https://lsdolab.github.io/lsdo-publications/publication/wang2025large/

```
@inproceedings{wang2025large,
  author = {Bingran Wang and Marius L. Ruh and Aoran Tian and Luca Scotzniovsky and John
    T. Hwang},
  title = {Large-scale MDO under uncertainty of an eVTOL aircraft using dimension
    reduction via global sensitivity analysis},
  booktitle = {AIAA AVIATION FORUM AND ASCEND 2025},
  year = {2025},
  doi = {10.2514/6.2025-3344},
  url = {https://doi.org/10.2514/6.2025-3344}
}
```

# Large-scale MDO under uncertainty of an eVTOL aircraft using dimension reduction via global sensitivity analysis

Bingran Wang*, Marius L. Ruh†, Aoran Tian‡, Luca Scotzniovsky§ and John T. Hwang¶
*University of California, San Diego, La Jolla, CA, 92093*

**Electric vertical takeoff and landing (eVTOL) aircraft have gained significant attention from both industry and academia due to their potential to transform urban transportation and promote sustainability through zero-emission propulsion. Recent work has demonstrated the effectiveness of multidisciplinary design optimization (MDO) in enhancing eVTOL performance at the conceptual design stage. However, most existing studies have focused on deterministic MDO problems neglecting the impact of real-world uncertainties. To address this gap, we formulate and demonstrate the solution of the first large-scale MDO under uncertainty (MDOUU) problem for NASA's Lift-Plus-Cruise configuration. This problem encompasses 51 design variables and 7 independent uncertain inputs. To keep the computational cost tractable, we introduce a novel sensitivity analysis-based, shared-grid uncertainty quantification framework that (i) screens each quantity of interest (QoI) with first-order Sobol indices and (ii) evaluates the resulting low-dimensional quadrature rules on a single, unioned node set. Numerical results demonstrate that the proposed UQ strategy achieves accurate statistical estimates for all 7 MDOUU quantities of interest (QoIs), with errors all below 5% using only 9 model evaluations. This strategy enables the efficient solution of the MDOUU problem, resulting in a reduction of 10.4% in aircraft empty weight compared to a baseline MDO design that is optimized using conservative safety factors.**

Author version · cite the published paper: doi.org/10.2514/6.2025-3344

## I. Introduction

Modern aerospace systems, such as aircraft, spacecraft, and advanced air mobility vehicles, demand high levels of performance, efficiency, and reliability across multiple tightly coupled physical disciplines. Multidisciplinary design optimization (MDO) has become an essential computational framework for systematically improving the designs of such systems by coupling analyses across disciplines such as aerodynamics, structures, propulsion, controls, and acoustics. MDO frameworks rely on numerical optimization algorithms to improve existing designs and allow engineers to explore complex trade-offs between competing objectives and constraints, yielding more effective and integrated engineering solutions [1–6]. One emerging application area for MDO is the design of electric vertical takeoff and landing (eVTOL) aircraft. These vehicles have attracted significant attention due to their potential to revolutionize regional air mobility with low-emission, low-noise vertical flight. The design of eVTOL aircraft requires careful coordination across propulsion, aerodynamics, structural weight, battery performance, and acoustics—making it an ideal testbed for MDO methodologies [7–12].

Current multidisciplinary design optimization (MDO) software such as OpenMDAO [13] and CSDL [14] typically employ a gradient-based approach to solve the numerical optimization problems. This approach analytically computes gradients and utilizes gradient-based optimization methods to enable efficient solutions for large-scale problems (with 100s or more of design variables) [15]. Despite the advances in MDO techniques and tools, most MDO studies on aerospace system only focus on determistic problems, ignoring the inherent uncertainties present in real-world operations. Variability in ambient conditions, payload mass, battery aging, aerodynamic coefficients, and manufacturing tolerances can lead to degraded performance or even mission failure if not properly accounted for during design. As a result, there is a growing recognition of the need to incorporate uncertainty quantification (UQ) into the MDO process to ensure robust and reliable designs [16, 17]. This motivates the framework of MDO under uncertainty (MDOUU), where performance metrics are treated as random variables and optimization is performed over their statistical moments or risk

*Postdoctoral Scholar, Department of Mechanical and Aerospace Engineering, AIAA Member.
†Ph.D Candidate, Department of Mechanical and Aerospace Engineering, AIAA Student Member.
‡M.S. Student, Department of Mechanical and Aerospace Engineering, AIAA Student Member.
§Ph.D Candidate, Department of Mechanical and Aerospace Engineering, AIAA Student Member.
¶Associate Professor, Department of Mechanical and Aerospace Engineering, AIAA Member.

measures. While this approach improves the robustness and reliability of the optimziation solutions, it significantly increases computational cost, as the statistical quantities and risk measures must be evaluated—typically through sampling or numerical integration—at every optimization iteration for solving the MDOUU problems. A 2002 NASA white paper identified the lack of efficient uncertainty-propagation techniques as a critical barrier to practical aerospace MDOUU [18]. To reduce the computational cost of MDOUU or general OUU problems, various methods have been proposed. These include:

- Surrogate modeling-based methods to reduce the number of expensive simulations [19, 20].
- Polynomial chaos expansion(PCE)-based methods to efficiently solve the UQ problems with minimum number of evaluations [21–23].
- Graph-accelerated UQ methods exploit the sparsity of multidisciplinary models to accelerate uncertainty propagation [24–27].
- Dimension-reduction techniques to isolate the most significant uncertain inputs to reduce the cost of UQ [28].

In this paper, we present an aggressive and scalable UQ framework for multi-output systems that integrates global-sensitivity-based dimension reduction with quadrature-based UQ methods. The key idea is to exploit the sparsity in input–output sensitivity revealed by Sobol indices: most outputs are significantly affected by only a small subset of uncertain variables. Based on this observation, we employ a shared-grid evaluation strategy and apply quadrature-based UQ methods tailored to each output. This enables efficient and accurate estimation of statistical moments using extremely few model evaluations, making the approach well-suited for large-scale MDOUU problems. We apply the proposed method to a practical large-scale MDOUU problem involving the NASA Lift-Plus-Cruise eVTOL configuration, which includes 51 design variables and 7 uncertain input parameters. Numerical results show that the proposed strategy can estimate all 7 MDOUU quantities of interest (QoIs) with less than 5% error using only 9 model evaluations. Furthermore, incorporating this method into the optimization loop enabled the successful solution of the MDOUU problem, resulting in a 10% reduction in aircraft weight compared to an MDO result that relies on a traditional safety factor approach.

The remainder of this paper is organized as follows. Section II reviews related work in UQ and MDOUU. Section III presents the proposed UQ method. Section IV introduces the eVTOL configuration and defines the optimization problem. Section V reports the numerical results and compares nominal MDO, safety-factor-based MDO, and MDOUU outcomes. Finally, Section VI summarizes key findings and outlines directions for future work.

## II. Background

### A. Multidisciplinary design optimization under uncertainty

We begin by considering a deterministic *multidisciplinary design optimization (MDO)* problem formulated using the *multidisciplinary feasible (MDF)* architecture. In this formulation, the state variables—such as aerodynamic forces, structural displacements, or thermal states—are not treated as optimization variables. Instead, they are implicitly solved by satisfying the residual equations at every model evaluation. This approach reduces the number of optimization variables and eliminates the need for additional optimization equality constraints, except those depending solely on the design variables. Under the MDF framework, we write the MDO problem as:

$$\begin{aligned} \min_{x} \quad & \mathcal{F}(x) \\ \text{subject to} \quad & C(x) < 0, \end{aligned} \tag{1}$$

where $x \in \mathbb{R}^n$ is the vector of design variables, $\mathcal{F}(x)$ denotes the objective function, and $C(x)$ represents the vector of inequality constraints. A detailed survey of MDO architectures, including MDF and its alternatives, can be found in [29]. The MDF formulation is particularly convenient for extending to *MDO under uncertainty (MDOUU)*, because the absence of state-based equality constraints avoids complications that arise when those outputs are affected by uncertain inputs. In practical engineering problems, various sources of uncertainty—such as ambient conditions, manufacturing variability, or operational disturbances—can influence the performance metrics defined by $\mathcal{F}$ and $C$. When such uncertainties are introduced, the deterministic formulation in Eq. (1) becomes invalid, as the objective and constraints become random variables.

To address this, the MDOUU problem can be formulated in a robust design optimization framework, where the

Author version · cite the published paper: doi.org/10.2514/6.2025-3344

objective and constraint functions are expressed in terms of their statistical moments:

$$\begin{aligned} \min_{x} \quad & \mathcal{M}(x) := \mathbb{E}[\mathcal{F}(x,U)] + \alpha_1 \mathbb{S}[\mathcal{F}(x,U)] \\ \text{subject to} \quad & \mathcal{N}(x) := \mathbb{E}[C(x,U)] + \alpha_2 \mathbb{S}[C(x,U)] < 0, \end{aligned} \tag{2}$$

Here, $U \in \mathbb{R}^d$ represents the vector of uncertain inputs, and $\mathbb{E}[\cdot]$ and $\mathbb{S}[\cdot]$ denote the expectation and standard deviation, respectively. The parameters $\alpha_1$ and $\alpha_2$ are user-defined weights that control the trade-off between performance and robustness in the objective and constraint functions. Alternatively, one may employ reliability-based constraints, where the goal is to ensure that the probability of constraint satisfaction exceeds a specified threshold.

When solving the MDOUU problem in Eq. (2) using a gradient-based optimizer, each design iteration requires the evaluation of the statistical quantities $\mathcal{M}(x)$ and $\mathcal{N}(x)$, along with their gradients $\frac{d\mathcal{M}}{dx}$ and $\frac{d\mathcal{N}}{dx}$. These evaluations typically rely on an embedded *uncertainty quantification (UQ)* solver to propagate uncertainty through the multidisciplinary system. The comparison between the computational frameworks for solving MDO and MDOUU problems are illustrated in Fig. 1.

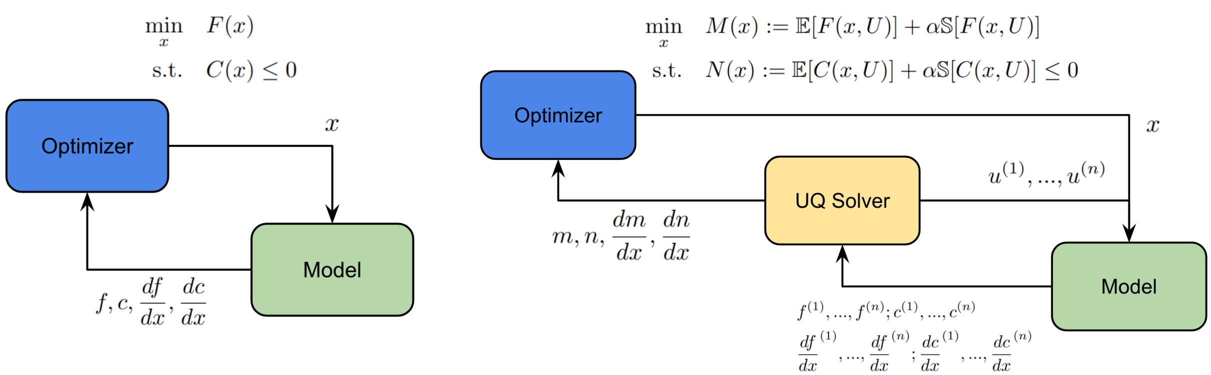


**Fig. 1 Computational frameworks for solving MDO and MDOUU problems using gradient-based optimizers [30]**

### B. Quadrature-based uncertainty quantification methods

The double-loop framework inherent in solving MDOUU problems introduces significant computational challenges, making the large-scale MDOUU problems computationally infeasible in many cases. This necessitates the use of highly efficient UQ methods to make large-scale MDOUU tractable in practical settings. In the MDOUU context, the UQ problem that needs to be solved during each optimization iteration is a forward UQ problem. In the single-output scenario, this involves evaluating a scalar-valued function subject to input uncertainties:

$$f = \mathcal{F}(u), \tag{3}$$

where $\mathcal{F} : \mathbb{R}^d \to \mathbb{R}$ is the deterministic model, $u \in \mathbb{R}^d$ is the vector of input parameters, and $f \in \mathbb{R}$ is the scalar output. The inputs are modeled as independent random variables, forming a stochastic input vector $U := [U_1, \ldots, U_d]$ with joint probability density function $\rho(u)$ supported on $\Gamma \subset \mathbb{R}^d$. The objective of the UQ problem is to compute the statistical moments of the output random variable $f(U)$.

In robust design optimization settings, where only the statistical moments (e.g., mean and variance) of the outputs are of interest, quadrature-based UQ methods—such as direct quadrature and quadrature-based non-intrusive polynomial chaos (NIPC) [31]—can be particularly effective for problems with low-dimensional uncertain inputs. These methods estimate the statistical moments by directly approximating the multi-dimensional integrals that define them. For instance, using direct quadrature, the first two moments of the output can be expressed as:

$$\begin{aligned} \mathbb{E}[f(U)] &= \int_\Gamma \mathcal{F}(u)\,\rho(u)\,du, \\ \mathrm{Var}[f(U)] &= \int_\Gamma (\mathcal{F}(u) - \mathbb{E}[f(U)])^2\,\rho(u)\,du. \end{aligned} \tag{4}$$



Author version · cite the published paper: doi.org/10.2514/6.2025-3344

These integrals can be approximated using numerical quadrature rules. For example, employing a tensor-product Gauss quadrature rule, the mean of the output is approximated as:

$$\begin{aligned}\mathbb{E}[f(U)] &= \int_{u_1} \dots \int_{u_d} f(u_1, \dots, u_d)\, \rho(u_1, \dots, u_d)\, du_1 \dots du_d \\ &\approx \sum_{i_1=1}^{k} \dots \sum_{i_d=1}^{k} w_1^{(i_1)} \dots w_d^{(i_d)}\, f(u_1^{(i_1)}, \dots, u_d^{(i_d)}),\end{aligned} \tag{5}$$

where $\{u_i^{(j)}\}_{j=1}^{k}$ and $\{w_i^{(j)}\}_{j=1}^{k}$ denote the nodes and weights of the 1D Gauss quadrature rule for the $i$-th input variable. A quadrature rule with $k$ points per dimension exactly integrates univariate polynomials up to degree $(2k-1)$. In the multi-dimensional setting, the full tensor-product quadrature rule evaluates the model at all combinations of univariate quadrature nodes:

$$\boldsymbol{u} = \boldsymbol{u}_1^k \times \cdots \times \boldsymbol{u}_d^k, \quad \text{where} \quad \boldsymbol{u}_i^k := \{u_i^{(j)}\}_{j=1}^{k}. \tag{6}$$

The total number of quadrature points is $k^d$, which grows exponentially with the number of uncertain inputs $d$. This exponential growth severely limits the applicability of full tensor-product quadrature methods to problems with only a small number of uncertain parameters (typically $d \leq 3$). To alleviate this limitation, sparse-grid quadrature and designed quadrature [32] methods can be used to reduce the number of required model evaluations while losing minimal accuracy.

Author version · cite the published paper: doi.org/10.2514/6.2025-3344

# III. Methodology

In this section, we introduce a global sensitivity-based UQ strategy to efficiently solve multidisciplinary design optimization under uncertainty (MDOUU) problems. The key idea is to leverage global sensitivity analysis to identify low-dimensional active subspaces in the space of uncertain inputs for each output of interest, and use a shared tensor-grid evaluation strategy to simultaneously solve the UQ problems for each quantity of interest (QoI) using the quadrature-based UQ methods.

In a typical MDOUU problem, the embedded forward UQ tasks are to evaluate the statistical moments or risk measures of multiple model outputs, which correspond to the objective and constraint functions in the optimization formulation. These outputs generally depend on a high-dimensional set of uncertain inputs, reflecting the multidisciplinary nature of the system. However, not all uncertain inputs contribute equally to the variability of each output. In practice, each output is often significantly influenced by only a small subset of the uncertain inputs, while being largely insensitive to the rest. Moreover, the subsets of influential inputs can differ across outputs, resulting in output-specific sensitivity patterns. This observation motivates the use of a global sensitivity-based strategy to perform output-specific dimension reduction. By identifying the dominant uncertain inputs that strongly influence each scalar output, we can construct low-dimensional quadrature rules tailored to each function. Furthermore, by leveraging a shared tensor-grid evaluation strategy, the multi-output UQ problem can be solved with high accuracy using only a small number of model evaluations. This makes the approach particularly powerful and scalable for solving large-scale MDOUU problems.

We begin by performing global sensitivity analysis (e.g., via Sobol indices) to quantify the impact of each uncertain input on each model output. For a model output $f_i(U)$, we rank the inputs $U_1, \dots, U_d$ based on their contribution to the variance of $f_i$. For each output, we retain only the top $r_i$ uncertain variables that dominate the output's variance. Typically, $r_i$ is small (e.g., 1–2), reflecting the sparsity in the input–output sensitivity structure. The remaining inputs, which exhibit negligible influence, are fixed at nominal values. This yields a reduced-dimension UQ problem for each output:

$$\tilde{f}_i = f_i(u_{(i,1)}, \dots, u_{(i,r_i)}), \tag{7}$$

where $u_{(i,j)}$ denotes the $j$-th most important uncertain variable for output $f_i$.

For each reduced-dimension output function $\tilde{f}_i$, we construct a tensor-product quadrature grid using Gauss quadrature rules. Since each output depends on a different subset of uncertain inputs, the corresponding quadrature grids are defined over different subspaces of the full uncertain input space. To avoid the inefficiency of solving each reduced UQ problem in isolation, we exploit the observation that the remaining inputs (those not in the dominant set for $f_i$) have negligible effect on $\tilde{f}_i$. As such, we can employ a *shared-grid evaluation* approach, which combines the quadrature grids from all outputs into a single evaluation batch by forming the union of the active quadrature points across outputs. Let

$Q_i$ be the set of quadrature points for output $f_i$, defined over its active subspace. The combined quadrature set is then:

$$Q_{\text{all}} = \bigcup_{i=1}^{N_{\text{outputs}}} \text{Lift}(Q_i), \tag{8}$$

where $\text{Lift}(Q_i)$ denotes the mapping of the reduced-dimension quadrature grid into the full $d$-dimensional input space by assigning nominal values to inactive inputs.

With the lifted quadrature points $Q_{\text{all}}$, we evaluate the full simulation model at each point and collect the responses for all outputs of interest. Since each quadrature grid only varies along the dominant subspace for its associated output, this strategy preserves quadrature accuracy while drastically reducing the total number of model evaluations compared to a full tensor-product rule in the original $d$-dimensional space. This method allows the computational cost to scale with the maximum reduced dimension $r_i$ across outputs, rather than with the full uncertain input dimension $d$. Moreover, it enables efficient reuse of model evaluations across multiple outputs, further improving the scalability of the approach.

### A. Illustrative example of shared quadrature evaluation

To demonstrate how the proposed shared quadrature evaluation method works, we consider a simplified problem with three uncertain inputs and three scalar outputs:

$$\begin{bmatrix} f_1 \\ f_2 \\ f_3 \end{bmatrix} = \mathcal{F}(u_1, u_2, u_3). \tag{9}$$

Let the uncertain input vector be $U = [U_1, U_2, U_3]$, where each $U_i$ is independent. The three outputs are denoted as $f_1(U)$, $f_2(U)$, and $f_3(U)$, and each output is assumed to be only significantly impacted by a lower-dimensional subset of the uncertain inputs:

- $f_1(U)$ is only significantly impacted by $U_1$ and $U_2$
- $f_2(U)$ is only significantly impacted by $U_2$ and $U_3$
- $f_3(U)$ is only significantly impacted by $U_3$

We use a 2-point Gauss quadrature rule in each input dimension. Let $u_i^{(1)}$ and $u_i^{(2)}$ denote the 1st and 2nd quadrature nodes in the $U_i$ dimension, and $w_i^{(1)}$ and $w_i^{(2)}$ denote the corresponding weights.

**Naive strategy:** A naive strategy would evaluate the UQ problem for each output independently using tensor-product quadrature:

- $f_1$: $2 \times 2$ tensor-grid evaluations in $(U_1, U_2) \Rightarrow 4$ points
- $f_2$: $2 \times 2$ tensor-grid evaluations in $(U_2, U_3) \Rightarrow 4$ points
- $f_3$: 2 tensor-grid evaluations in $U_3 \Rightarrow 2$ points

This requires a total of $4 + 4 + 2 = 10$ model evaluations.

**Shared-grid evaluation strategy:** Instead of evaluating each quadrature grid separately, we propose a shared evaluation strategy to stack the required variations along active directions to form a small set of shared quadrature points that collectively cover all necessary quadrature projections. The key observation is that each output is insensitive to certain inputs, allowing us to combine quadrature nodes efficiently. The resulting shared quadrature point set is:

$$Q_{\text{shared}} = \left\{ \begin{array}{c} \left(u_1^{(1)}\right) \\ \left(u_1^{(2)}\right) \\ \left(u_1^{(3)}\right) \\ \left(u_1^{(4)}\right) \end{array} \right\} = \left\{ \begin{array}{c} \left(u_1^{(1)}, u_2^{(1)}, u_3^{(1)}\right) \\ \left(u_1^{(1)}, u_2^{(2)}, u_3^{(2)}\right) \\ \left(u_1^{(2)}, u_2^{(1)}, \bar{u}_3\right) \\ \left(u_1^{(2)}, u_2^{(2)}, \bar{u}_3\right) \end{array} \right\},$$

where $\bar{u}_3$ denotes the nominal value of $U_3$. This shared set ensures that:

- $f_1$ sees all combinations of $(U_1, U_2)$
- $f_2$ sees all combinations of $(U_2, U_3)$
- $f_3$ sees both $U_3$ quadrature points



Author version · cite the published paper: doi.org/10.2514/6.2025-3344

**Table 1 Shared quadrature points and corresponding weights for each output**

| | Quadrature points | | | Weights | | |
|---|---|---|---|---|---|---|
| $U$ | $U_1$ | $U_2$ | $U_3$ | $f_1$ | $f_2$ | $f_3$ |
| $u^{(1)}$ | $u_1^{(1)}$ | $u_2^{(1)}$ | $u_3^{(1)}$ | $w_1^{(1)} w_2^{(1)}$ | $w_2^{(1)} w_3^{(1)}$ | $w_3^{(1)}$ |
| $u^{(2)}$ | $u_1^{(1)}$ | $u_2^{(2)}$ | $u_3^{(2)}$ | $w_1^{(1)} w_2^{(2)}$ | $w_2^{(2)} w_3^{(2)}$ | $w_3^{(2)}$ |
| $u^{(3)}$ | $u_1^{(2)}$ | $u_2^{(1)}$ | $\bar{u}_3$ | $w_1^{(2)} w_2^{(1)}$ | $w_2^{(1)} w_3^{(2)}$ | 0 |
| $u^{(4)}$ | $u_1^{(2)}$ | $u_2^{(2)}$ | $\bar{u}_3$ | $w_1^{(2)} w_2^{(2)}$ | $w_2^{(2)} w_3^{(1)}$ | 0 |

The quadrature weights associated with these points are shown in Table 1. The proposed strategy reduces the total number of model evaluations from 10 to only 4, while preserving the ability to accurately compute statistical moments for all three outputs using low-dimensional quadrature projections.

### B. Automated axis selection for tensor-grid quadrature points

When the number of random inputs or outputs grows into the dozens or hundreds, manually deciding which variables should share each tensor–grid axis becomes infeasible. We therefore cast *axis selection* as a one-time binary-assignment problem. Let $d$ be the number of random inputs, $m$ be the number of QoIs (outputs), and $k$ be the number of global sampling axes in the tensor-product quadrature rule ($k \ll d$). The goal is to map the $d$ random inputs onto a much smaller set of $k$ global sampling axes based on output-specific sensitivities in such a way that no single scenario has more than one influential input assigned to the same axis. This requirement ensures that the resulting tensor grid retains its low effective dimension for every scenario we must analyze. We start with a sensitivity matrix

$$S \in \{0,1\}^{d\times m}$$

which can be generated based on the sensitivity analysis results. Its entry $s_{ij}$ equal to 1 indicates output $j$ is significantly influenced by input $i$ and equal to 0 otherwise. We seek a binary assignment matrix $A \in \{0,1\}^{d\times k}$, where $A_{i\ell} = 1$ indicates that random input $i$ varies along global axis $\ell$. The optimal assignment is obtained from the integer linear programming problem:

$$\begin{aligned} &\min_{A} \mathbf{1}_d^{\mathsf{T}}(A \odot W)\mathbf{1}_k && \text{(for unique solution)} \\ &\text{s. t. } A\mathbf{1}_k = \mathbf{1}_d && \text{(unique axis assignment)} \\ &\quad A^{\mathsf{T}} S \le \mathbf{1}_{k\times m} && \text{(no output sees a conflict)} \\ &\quad A \in \{0,1\}^{d\times k}. \end{aligned} \tag{ILP}$$

Here $\mathbf{1}_d$ and $\mathbf{1}_k$ are all-ones vectors and $\odot$ denotes element-wise multiplication. The weight matrix $W \in \mathbb{R}_+^{d\times k}$ is arbitrarily chosen to ensure unique solution (e.g. each element can be arbitrarily chosen to be between 0 and 1).

When choosing $k$, one should begin with $k_{\min} = \max_j \sum_i S_{ij}$, the greatest number of influential inputs that ever appear in the same output. If (ILP) is infeasible at $k = k_{\min}$, increment $k$ until a feasible assignment is found. In practice only one or two extra axes are needed. The $A$ matrix can subsequently be used to determine the shared-grid quadrature points, $Q_{\text{shared}}$, and the corresponding weights to solve for the multi-output UQ problem.

## IV. Problem set-up

This study focuses on the system-level design optimization of the NASA Lift-Plus-Cruise Urban Air Mobility (UAM) reference vehicle [33]. The vehicle features a distributed electric propulsion architecture with eight lift rotors used during vertical flight phases (e.g., hover and takeoff) and a single pusher propeller for forward flight, where the vehicle operates as a fixed-wing aircraft. The propulsion architecture is fully electric, though a hybrid version was also proposed by NASA [33].

Author version · cite the published paper: doi.org/10.2514/6.2025-3344

We consider a large-scale multidisciplinary design optimization (MDO) problem based on the formulation presented in [34]. In our study, we consider a reduced mission profile that includes three key flight segments: hover, climb, and cruise. These segments dominate the power and energy requirements of the mission and are essential for propulsion and battery sizing. The full mission profile is illustrated in Fig. 2, and the main modeling disciplines included in the computational model are summarized in Fig. 3. We note that for comprehensive analysis, it is important to also consider off-design sizing conditions (e.g., motor failure or structural sizing) as well as a more detailed mission profile that includes a transition maneuver. However, due to the increased complexity, solving a problem of this scale while considering randomness is outside the scope of this study.

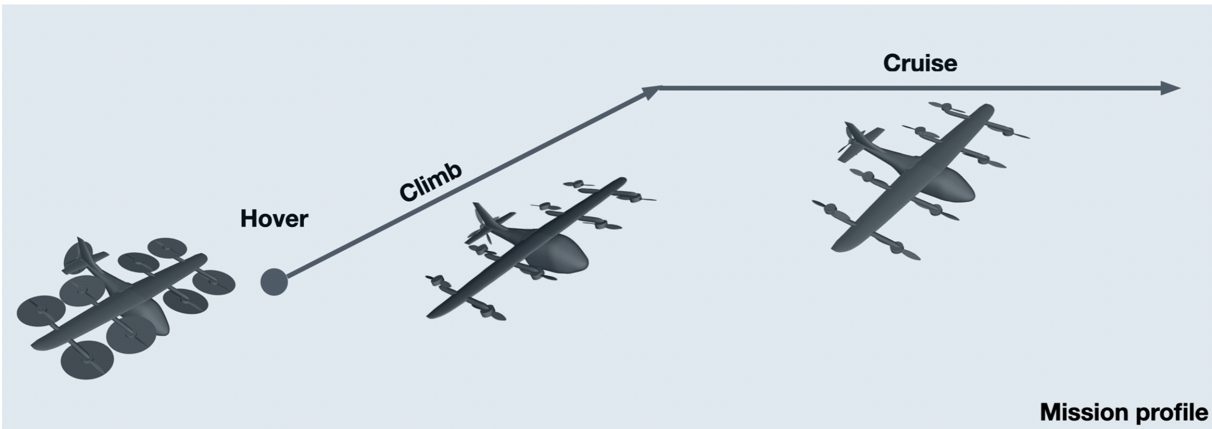


**Fig. 2 Full mission profile of the NASA Lift-Plus-Cruise reference eVTOL vehicle (figure adopted from [34])**

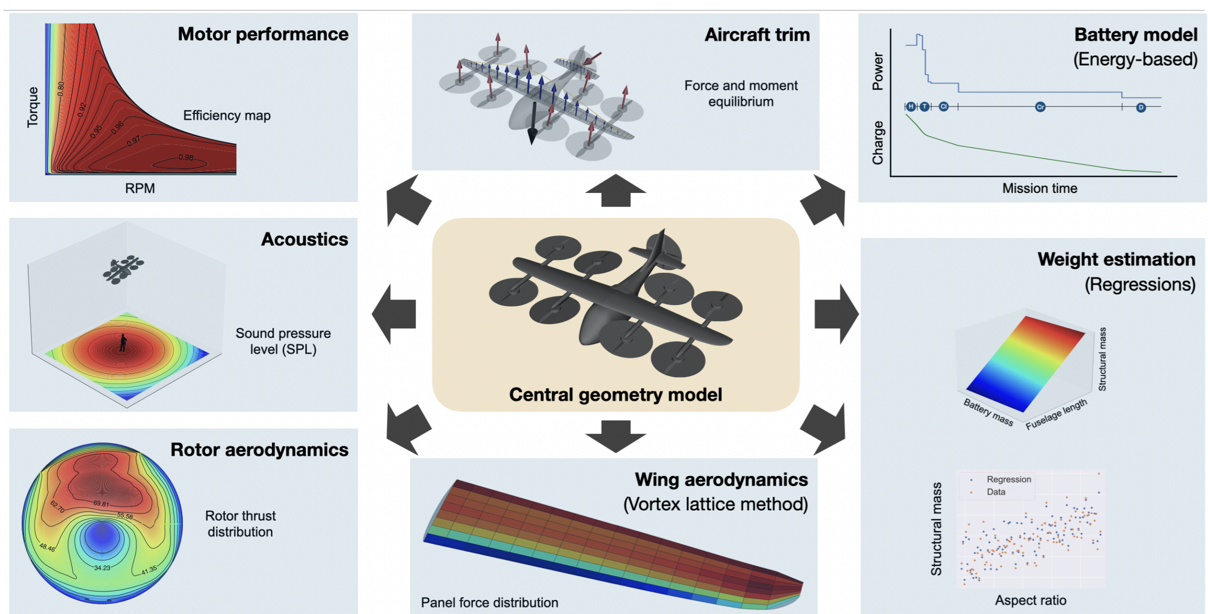


**Fig. 3 Key disciplines considered in the eVTOL design optimization problem (figure adopted from [34])**

Our computational model integrates low-fidelity physics-based analyses for aerodynamics (vortex lattice method), rotor and propeller performance (blade element momentum theory), aeroacoustics (tonal and broadband noise), motor performance (equivalent circuit model), battery modeling (energy-based sizing), and aircraft trim (force and moment equilibrium). These models are connected to a high-fidelity central geometry model that uses free-form deformation (FFD) to update solver meshes during design optimization. We refer the reader to Ruh et al. [10, 34] for more information regarding the physics-based models used in this study and the parameterization of the central geometry. These models



Author version · cite the published paper: doi.org/10.2514/6.2025-3344

collectively capture the key first-order interactions that govern aircraft performance and feasibility across mission segments. This setup allows us to formulate a representative MDO problem that captures the dominant sizing drivers while maintaining computational tractability. Modeling higher-order effects like rotor-wing interactions or structural failure modes are outside the scope of this paper. The MDO problem formulation is provided in Tab. 2. Our objective here is to minimize the aircraft's empty weight while satisfying mission and design constraints, including those related to aircraft trim, battery energy capacity, motor torque margins, and geometric feasibility. The design variables span several physical subsystems and include:

- Geometric parameters: wing and tail planform areas, aspect ratios, and fuselage length
- Propulsion parameters: rotor radii and motor sizing variables
- Energy storage: battery mass

**Table 2 MDO problem formulation**

| | Description | Range (units) | Quantity |
|---|---|---|---|
| Objective | Aircraft empty weight | $W$ (kg) | 1 |
| Constraints | Hover total noise | $SPL < 70$ (dB) | 1 |
| | Battery final state of charge | $SoC > 20\%$ | 1 |
| | Motor torque safety margin | $T_d > 10\%$ | 5 |
| | | | Total constraints: 7 |
| Design variables | Wing aspect ratio | $\mathbf{AR}_{\text{wing}}$ | 1 |
| | Tail aspect ratio | $\mathbf{AR}_{\text{tail}}$ | 1 |
| | Wing planform area | $\mathbf{S}_{\text{wing}}$ | 1 |
| | Tail planform area | $\mathbf{S}_{\text{tail}}$ | 1 |
| | Fuselage length | $\mathbf{L}_{\text{fuselage}}$ | 1 |
| | Blade chord ($5 \times 4$) | $\mathbf{C}_{\text{blade}}$ | 20 |
| | Blade twist ($5 \times 4$) | $\mathbf{T}_{\text{blade}}$ | 20 |
| | Blade radius | $\mathbf{R}_{\text{blade}}$ | 5 |
| | Battery Mass | $\mathbf{m}_{\text{battery}}$ | 1 |
| | | | Total design variables: 51 |

### A. MDOUU formulation

From the perspective of eVTOL aircraft design, we identify seven key independent uncertain inputs to capture representative sources of variability across the operational, design, and manufacturing domains. The resulting MDOUU problem, summarized in Table 2, includes mission-level uncertainties such as hover altitude, cruise altitude, climb Mach number, and cruise Mach number; system-level uncertainty such as payload weight; and component-level manufacturing variability, namely motor slenderness ratio and motor torque density. This selection is motivated by the significant impact these variables have on aircraft performance and constraint feasibility. Operational uncertainties—such as those in flight altitude and Mach number—introduce variability in aerodynamic loads and propulsion requirements. Payload mass variability reflects differences in passenger or cargo weight, while manufacturing tolerances in motor properties affect torque capability and overall system feasibility.

Importantly, the aircraft empty weight—used as the objective function—is only a function of the design variables and is therefore unaffected by these uncertain inputs. In contrast, the constraints (e.g., noise, battery state of charge, and torque margins) are directly influenced by the random variables. To incorporate uncertainty into constraint evaluation, we adopt a robust design optimization formulation, where constraints are treated probabilistically using moment-based approximations. Specifically, each constraint is enforced based on its mean and standard deviation, using a conservative margin defined by the form $\mu \pm \alpha\sigma$, ensuring high-probability feasibility under uncertainty.

Author version · cite the published paper: doi.org/10.2514/6.2025-3344

**Table 3 MDOUU problem formulation**

| | Description | Range (units) | Quantity |
|---|---|---|---|
| Objective | Aircraft empty weight | $W$ (kg) | 1 |
| Constraints | Hover total noise | $\mu_{SPL} + 3\sigma_{SPL} < 70$ (dB) | 1 |
| | Battery final state of charge | $\mu_{SoC} - 3\sigma_{SoC} > 20\%$ | 1 |
| | Motor torque safety margin | $\mu_{T_d} - 3\sigma_{T_d} > 10\%$ | 5 |
| | | | Total constraints: 7 |
| Design variables | Wing aspect ratio | $\mathbf{AR}_{\text{wing}}$ | 1 |
| | Tail aspect ratio | $\mathbf{AR}_{\text{tail}}$ | 1 |
| | Wing planform area | $\mathbf{S}_{\text{wing}}$ | 1 |
| | Tail planform area | $\mathbf{S}_{\text{tail}}$ | 1 |
| | Fuselage length | $\mathbf{L}_{\text{fuselage}}$ | 1 |
| | Blade chord ($5 \times 4$) | $\mathbf{C}_{\text{blade}}$ | 20 |
| | Blade twist ($5 \times 4$) | $\mathbf{T}_{\text{blade}}$ | 20 |
| | Blade radius | $\mathbf{R}_{\text{blade}}$ | 5 |
| | Battery Mass | $\mathbf{m}_{\text{battery}}$ | 1 |
| | | | Total design variables: 51 |
| Random variables | Hover altitude | $\mathcal{U}(80, 120)$ (m) | 1 |
| | Cruise altitude | $\mathcal{U}(800, 1200)$ (m) | 1 |
| | Climb mach number | $\mathcal{U}(0.14, 0.22)$ | 1 |
| | Cruise mach number | $\mathcal{U}(0.14, 0.22)$ | 1 |
| | Payload weight | $\mathcal{U}(440, 640)$ (kg) | 1 |
| | Motor slenderness ratio | $\mathcal{N}(0.3, 0.03)$ | 1 |
| | Motor torque density | $\mathcal{N}(30, 3)$ (Nm/kg) | 1 |
| | | | Total random variables: 7 |

# V. Numerical results

This section presents the numerical evaluation of the proposed method. Specifically, we (i) validate the accuracy and efficiency of the proposed dimension-reduced uncertainty quantification (UQ) strategy, (ii) quantify its impact on multidisciplinary design optimization under uncertainty (MDOUU) results, and (iii) discuss the resulting design insights.

## A. Global sensitivity analysis

The first-order Sobol indices are approximated following [35] using first order derivatives. The results are listed in Tab. 4 and visualised as a heat map in Fig. 4. They reveal an exceptionally sparse input–output dependence structure:

- **Hover noise** is governed almost exclusively by *hover altitude* (index = 1.00), confirming that atmospheric conditions dominate perceived acoustic levels in hover.
- **Final battery state-of-charge (SoC)** depends primarily on *cruise Mach number* (0.77) and, to a lesser extent, *cruise altitude* (0.20); all other inputs contribute $< 2\,\%$. This matches engineering intuition that cruise power is the largest energy draw of the mission.
- **Torque safety margins** for both pusher and lift rotors are controlled by the *motor slenderness ratio* ($> 0.96$), with a minor influence from *motor torque density* ($\sim 0.02$–$0.03$). Operating-condition uncertainties play no meaningful role because the motors are sized for worst-case thrust.

Because each quantity of interest (QoI) is sensitive to at most two of the seven random inputs, this justifies the use of our proposed aggressive UQ stratgegy to use a 2-order tensor grids to solve the multi-output UQ problem without appreciable information loss.



Author version · cite the published paper: doi.org/10.2514/6.2025-3344

**Table 4 First order Sobol indices results**

| | Input Variable | Final SoC | Hover noise | Torque safety margin (pusher rotor) | Torque safety margin (vertical rotor 1) |
|---|---|---|---|---|---|
| 1 | hover_altitude | 0.000 | 1.000 | 0.000 | 0.000 |
| 2 | cruise_altitude | 0.199 | 0.000 | 0.000 | 0.000 |
| 3 | climb_mach_number | 0.014 | 0.000 | 0.009 | 0.000 |
| 4 | cruise_mach_number | 0.769 | 0.000 | 0.000 | 0.000 |
| 5 | payload_mass | 0.017 | 0.000 | 0.000 | 0.000 |
| 6 | motor_slenderness_ratio | 0.000 | 0.000 | 0.964 | 0.974 |
| 7 | motor_torque_density | 0.000 | 0.000 | 0.026 | 0.026 |


**Fig. 4 First order Sobol indices heat map**

Author version · cite the published paper: doi.org/10.2514/6.2025-3344

### B. Accuracy of proposed UQ method

The proposed method is tested on estimating all of the MDOUU QoIs ($\mu \pm \alpha\sigma$) that are affected by the uncertain inputs. The results are presented in Tab. 5. The proposed shared quadrature evaluation method with $2 \times 2$, $3 \times 3$ and $4 \times 4$ grids are compared against a 2 000-sample Monte-Carlo reference. The results show that, even the smallest 2×2 grid (four model evaluations in total) reproduces the hover-noise metric to machine precision and keeps all other errors below ~13%. The 3×3 grid—our default choice in the optimization loop—requires only 9 model evaluations yet reduces the maximum error across all quantities of interest (QoIs) to $<5\%$, while the 4×4 grid drives every error below 3%.

Because each QoI depends on at most two dominant uncertain inputs, the full $3^7 = 2187$ points of a naive tensor Gauss grid collapse to at most $3^2 = 9$ points after dimension reduction—a 243× reduction in model calls per UQ solve. This order-of-magnitude saving is what enables an otherwise intractable large-scale MDOUU study.

### C. MDO versus MDO with safety factors versus MDOUU

Tab. 6 contrasts the optimal designs obtained with

- deterministic MDO evaluated at nominal conditions,
- deterministic MDO augmented with conventional safety factors,
- the proposed MDOUU formulation.

Table 5 **Comparison of MDOUU quantity of interest (QoI): $\mu \pm \alpha\sigma$ across methods. Relative errors (%) are with respect to Monte Carlo (2000 samples).**

| MDOUU QoI ($\mu \pm \alpha\sigma$) | MC (2000) | Our method | | |
|---|---|---|---|---|
| | | 2×2 grid | 3×3 grid | 4×4 grid |
| Final SoC | -0.0757 | -0.0706 (6.7%) | -0.0790 (4.4%) | -0.0711 (6.0%) |
| Hover Noise | 70.7948 | 70.7947 (<0.01%) | 70.7947 (<0.01%) | 70.7946 (<0.01%) |
| Torque safety margin (pusher rotor) | -1.2601 | -1.0998 (12.7%) | -1.2246 (2.8%) | -1.2760 (1.3%) |
| Torque safety margin (lift rotor 1) | -0.8690 | -0.7949 (8.5%) | -0.8803 (1.3%) | -0.8946 (2.9%) |

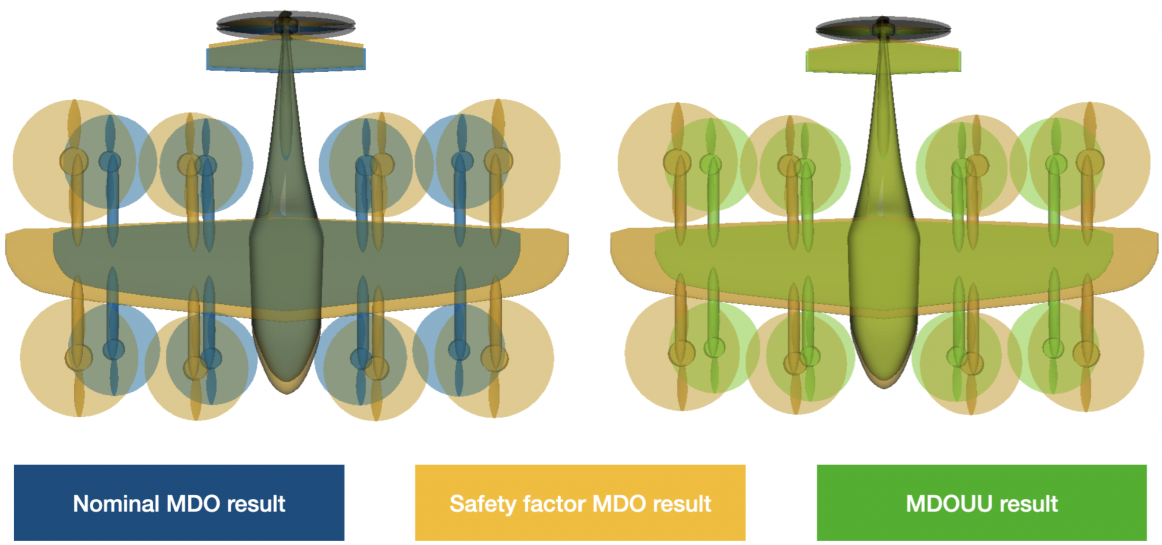


**Fig. 5 Visualizations of the MDO and MDOUU results**

The safety factors are chosen based on the UQ analysis results on the initial design. The safety-factor design incurs a 19% empty-weight penalty (3343 kg vs. 2814 kg) to suppress the > 100% average constraint violations observed in the nominal MDO solution. By explicitly accounting for the seven random variables, the MDOUU approach restores feasibility (< 1% mean violation) while cutting the empty weight to 3027 kg—**a 10.4% reduction** relative to the safety-factor design and only a 7.6% increase over the unconstrained nominal.

From the eVTOL aircraft design perspective, MDOUU recovers much of the lightweight wing planform, aspect-ratio, and rotor selection of the nominal optimum, but retains the enlarged battery and slight fuselage stretch required for robustness. In contrast, the safety-factor solution inflates both lifting-surface areas and rotor radii across the board, illustrating how coarse safety margins can drive the design into a sub-optimal corner of the feasible space. The visualizations of the MDO and MDOUU results are shown in 5.

## VI. Conclusion

This study proposes an aggressive, yet conceptually simple, uncertainty-quantification strategy that combines (i) global-sensitivity-based, output-specific dimension reduction with (ii) a shared-grid, tensor-quadrature evaluation scheme. By exploiting the remarkable sparsity revealed by first-order Sobol indices, each quantity of interest (QoI) can be reduced to a one- or two-dimensional integration problem, after which the lifted union of low-order Gauss grids allows all QoIs to be evaluated simultaneously with a handful of model calls. When embedded in a gradient-based multidisciplinary design-optimization-under-uncertainty (MDOUU) loop, this approach preserves adjoint-level efficiency and adds virtually no algorithmic complexity to existing MDO paradigms.

Applied to the NASA Lift-Plus-Cruise reference eVTOL, the method estimates the seven coupled MDOUU QoIs to within 5% using only nine model evaluations. The resulting MDOUU solution is 10.4% lighter than a conventional



Author version · cite the published paper: doi.org/10.2514/6.2025-3344

**Table 6 Comparison of MDO and MDOUU results**

| | MDO-optimized design (with nominal values) | MDO-optimized design (with safety factor) | MDOUU-optimized design |
|---|---|---|---|
| MAJOR DESIGN VARIABLES: | | | |
| Wing aspect ratio | 8.48 | 9.03 | 8.48 |
| Tail aspect ratio | 5.59 | 5.13 | 5.59 |
| Wing planform area [$m^2$] | 17.0 | 23.2 | 17.3 |
| Tail planform area [$m^2$] | 3.00 | 3.07 | 2.98 |
| Fuselage length [m] | 8.89 | 9.34 | 9.04 |
| Battery mass [kg] | 776 | 991 | 902 |
| Pusher rotor radius [m] | 1.78 | 1.78 | 1.78 |
| Front inner rotor radius [m] | 1.20 | 1.359 | 1.20 |
| Rear inner rotor radius [m] | 1.20 | 1.326 | 1.20 |
| Front outer rotor radius [m] | 1.20 | 1.541 | 1.22 |
| Rear outer rotor radius [m] | 1.20 | 1.574 | 1.22 |
| OBJECTIVE FUNCTIONS: | | | |
| Aircraft empty weight [kg] | 2814 | 3343 | 3027 |
| MDOUU CONS. VIOL.: | | | |
| Final SoC | > 30% | <1% | <1% |
| Hover noise | > 5% | 0% | 0% |
| Torque safety margin (pusher rotor) | > 400% | 0% | <1% |
| Torque safety margin (lift rotors) | > 400% | 0% | 0% |
| Avg. MDOUU cons. viol. | >100% | <1% | <1% |
| SAFETY FACTORS USED: | | | |
| Final SoC | - | 1.4 | - |
| Hover noise | - | 1.1 | - |
| Torque safety margin (pusher rotor) | - | 5 | - |
| Torque safety margin (lift rotors) | - | 5 | - |

safety-factor design and retains strict probabilistic feasibility (<1% average violation) with only a 7.6% weight penalty over an unconstrained deterministic optimum. These outcomes demonstrate that large-scale, industrial-fidelity eVTOL designs can now be optimized for robustness and performance on standard computing resources—a task previously viewed as impractical.

## Acknowledgments

The material presented in this paper is, in part, based upon work supported by NASA under award No. 80NSSC23M0217.

## References

[1] Kenway, G., and Martins, J. R., "Aerostructural shape optimization of wind turbine blades considering site-specific winds," *12th AIAA/ISSMO multidisciplinary analysis and optimization conference*, 2008, p. 6025. https://doi.org/10.2514/6.2008-6025.

[2] Balesdent, M., Bérend, N., Dépincé, P., and Chriette, A., "A survey of multidisciplinary design optimization methods in launch vehicle design," *Structural and Multidisciplinary optimization*, Vol. 45, No. 5, 2012, pp. 619–642. https://doi.org/10.1007/s00158-011-0701-4.

[3] Jilla, C., and Miller, D., "A multiobjective, multidisciplinary design optimization methodology for the conceptual design of



Author version · cite the published paper: doi.org/10.2514/6.2025-3344

distributed satellite systems," *9th AIAA/ISSMO Symposium on Multidisciplinary Analysis and Optimization*, 2002, p. 5491. https://doi.org/10.2514/6.2002-5491.

[4] Hwang, J. T., Lee, D. Y., Cutler, J. W., and Martins, J. R., "Large-scale multidisciplinary optimization of a small satellite's design and operation," *Journal of Spacecraft and Rockets*, Vol. 51, No. 5, 2014, pp. 1648–1663. https://doi.org/10.2514/1.a32751.

[5] Kaneko, S., and Martins, J. R., "Fleet design optimization of package delivery unmanned aerial vehicles considering operations," *Journal of Aircraft*, Vol. 60, No. 4, 2023, pp. 1061–1077.

[6] Orndorff, N. C., Wang, B., Ruh, M. L., Fletcher, A., and Hwang, J. T., "Gradient-based sizing optimization of power-beaming-enabled aircraft," *AIAA AVIATION 2023 Forum*, 2023, p. 4019. https://doi.org/10.2514/6.2023-4019.

[7] Brelje, B. J., and Martins, J. R., "Electric, hybrid, and turboelectric fixed-wing aircraft: A review of concepts, models, and design approaches," *Progress in Aerospace Sciences*, Vol. 104, 2019, pp. 1–19.

[8] Sarojini, D., Ruh, M. L., Joshy, A. J., Yan, J., Ivanov, A. K., Scotzniovsky, L., Fletcher, A. H., Orndorff, N. C., Sperry, M., Gandarillas, V. E., et al., "Large-Scale Multidisciplinary Design Optimization of an eVTOL Aircraft using Comprehensive Analysis," *AIAA SCITECH 2023 Forum*, 2023, p. 0146. https://doi.org/10.2514/6.2023-0146.

[9] van Schie, S. P., Ruh, M. L., Fletcher, A. H., Warner, M., Sperry, M., Scotzniovsky, L., Orndorff, N. C., Xiang, R., Yan, J., Zhao, H., et al., "Large-Scale Distributed Multidisciplinary Design Optimization of the NASA Lift-Plus-Cruise Air Taxi Concept," *AIAA SCITECH 2025 Forum*, 2025, p. 0362.

[10] Ruh, M. L., Sarojini, D., Fletcher, A., Asher, I., and Hwang, J. T., "Large-scale multidisciplinary design optimization of the NASA lift-plus-cruise concept using a novel aircraft design framework," *arXiv preprint arXiv:2304.14889*, 2023.

[11] Kaneko, S., and Martins, J. R., "Simultaneous optimization of design and takeoff trajectory for an eVTOL aircraft," *Aerospace Science and Technology*, Vol. 155, 2024, p. 109617.

[12] Shahjahan, S., Gong, A., Moore, A., and Verstraete, D., "Optimisation of proprotors for tilt-wing eVTOL aircraft," *Aerospace Science and Technology*, Vol. 144, 2024, p. 108835.

[13] Gray, J. S., Hwang, J. T., Martins, J. R., Moore, K. T., and Naylor, B. A., "OpenMDAO: An open-source framework for multidisciplinary design, analysis, and optimization," *Structural and Multidisciplinary Optimization*, Vol. 59, No. 4, 2019, pp. 1075–1104. https://doi.org/10.2514/6.2010-9101.

[14] Gandarillas, V., Joshy, A. J., Sperry, M. Z., Ivanov, A. K., and Hwang, J. T., "A graph-based methodology for constructing computational models that automates adjoint-based sensitivity analysis," *Structural and Multidisciplinary Optimization*, under revision.

[15] Hwang, J. T., "A modular approach to large-scale design optimization of aerospace systems," *Ph. D. thesis*, 2015.

[16] Meng, D., Yang, S., He, C., Wang, H., Lv, Z., Guo, Y., and Nie, P., "Multidisciplinary design optimization of engineering systems under uncertainty: a review," *International Journal of Structural Integrity*, Vol. 13, No. 4, 2022, pp. 565–593.

[17] Wang, B., Orndorff, N. C., Joshy, A. J., and Hwang, J. T., "Graph-accelerated large-scale multidisciplinary design optimization under uncertainty of a laser-beam-powered aircraft," *AIAA SCITECH 2024 Forum*, 2024, p. 0169.

[18] Zang, T. A., *Needs and opportunities for uncertainty-based multidisciplinary design methods for aerospace vehicles*, National Aeronautics and Space Administration, Langley Research Center, 2002.

[19] Rumpfkeil, M. P., "Optimizations under uncertainty using gradients, Hessians, and surrogate models," *AIAA journal*, Vol. 51, No. 2, 2013, pp. 444–451. https://doi.org/10.2514/1.J051847.

[20] Moustapha, M., Sudret, B., Bourinet, J.-M., and Guillaume, B., "Quantile-based optimization under uncertainties using adaptive Kriging surrogate models," *Structural and multidisciplinary optimization*, Vol. 54, 2016, pp. 1403–1421.

[21] Mishra, A. A., Mukhopadhaya, J., Alonso, J., and Iaccarino, G., "Design exploration and optimization under uncertainty," *Physics of Fluids*, Vol. 32, No. 8, 2020.

[22] Keshavarzzadeh, V., Fernandez, F., and Tortorelli, D. A., "Topology optimization under uncertainty via non-intrusive polynomial chaos expansion," *Computer Methods in Applied Mechanics and Engineering*, Vol. 318, 2017, pp. 120–147. https://doi.org/10.1016/j.cma.2017.01.019.

Author version · cite the published paper: doi.org/10.2514/6.2025-3344

[23] Lee, D., and Rahman, S., "Robust design optimization under dependent random variables by a generalized polynomial chaos expansion," *Structural and Multidisciplinary Optimization*, Vol. 63, No. 5, 2021, pp. 2425–2457.

[24] Wang, B., Sperry, M., Gandarillas, V. E., and Hwang, J. T., "Accelerating model evaluations in uncertainty propagation on tensor grids using computational graph transformations," *arXiv preprint arXiv:2309.06617*, 2023. https://doi.org/10.48550/arXiv.2309.06617.

[25] Wang, B., Orndorff, N. C., and Hwang, J. T., "Graph-accelerated non-intrusive polynomial chaos expansion using partially tensor-structured quadrature rules for uncertainty quantification," *Aerospace Science and Technology*, Vol. 155, 2024, p. 109607.

[26] Wang, B., Orndorff, N. C., Sperry, M., and Hwang, J. T., "Extension of graph-accelerated non-intrusive polynomial chaos to high-dimensional uncertainty quantification through the active subspace method," *Aerospace Science and Technology*, Vol. 160, 2025, p. 110074.

[27] Wang, B., Orndorff, N. C., Sperry, M., and Hwang, J. T., "A gradient-enhanced univariate dimension reduction method for uncertainty propagation," *AIAA SCITECH 2024 Forum*, 2024.

[28] Lee, I., Choi, K., Du, L., and Gorsich, D., "Dimension reduction method for reliability-based robust design optimization," *Computers & Structures*, Vol. 86, No. 13-14, 2008, pp. 1550–1562. https://doi.org/10.1016/j.compstruc.2007.05.020.

[29] Martins, J. R., and Lambe, A. B., "Multidisciplinary design optimization: a survey of architectures," *AIAA Journal*, Vol. 51, No. 9, 2013, pp. 2049–2075.

[30] Scotzniovsky, L., and Hwang, J., "A fast, memory-efficient panel method for large-scale multidisciplinary design optimization under uncertainty using graph-based modeling," *AIAA AVIATION 2025 Forum*, 2025.

[31] Xiu, D., and Karniadakis, G. E., "The Wiener–Askey polynomial chaos for stochastic differential equations," *SIAM journal on scientific computing*, Vol. 24, No. 2, 2002, pp. 619–644. https://doi.org/10.1137/S1064827501387826.

[32] Keshavarzzadeh, V., Kirby, R. M., and Narayan, A., "Numerical integration in multiple dimensions with designed quadrature," *SIAM Journal on Scientific Computing*, Vol. 40, No. 4, 2018, pp. A2033–A2061. https://doi.org/10.1137/17M1137875.

[33] Silva, C., Johnson, W. R., Solis, E., Patterson, M. D., and Antcliff, K. R., "VTOL urban air mobility concept vehicles for technology development," *2018 Aviation Technology, Integration, and Operations Conference*, 2018, p. 3847. https://doi.org/10.2514/6.2018-3847.

[34] Ruh, M., Warner, M., Luca, S., Andrew, F., Mark, S., and John, H., "System-Level large-scale multidisciplinary design optimization of an urban air mobility reference vehicle," *Journal of Aircraft*, under review.

[35] Sobol, I. M., and Kucherenko, S., "Derivative based global sensitivity measures and their link with global sensitivity indices," *Mathematics and Computers in Simulation*, Vol. 79, No. 10, 2009, p. 3009.

Author version · cite the published paper: doi.org/10.2514/6.2025-3344